

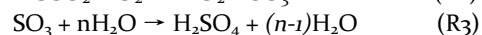
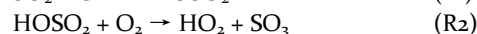
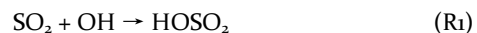
# Reaction of SO<sub>3</sub> with HONO<sub>2</sub> and Implications for Sulfur Partitioning

Bo Long,<sup>1</sup> Yu Xia,<sup>1</sup> Junwei Lucas Bao,<sup>2</sup> Javier Carmona-García,<sup>3,4</sup> Juan Carlos Gómez Martín,<sup>5</sup> John M. C. Plane,<sup>6</sup> Alfonso Saiz-Lopez,<sup>4</sup> Daniel Roca-Sanjuán,<sup>3</sup> Joseph S. Francisco,<sup>7\*</sup>

## Supporting Information Placeholder

**ABSTRACT:** Sulfur trioxide is a critical intermediate for the sulfur cycle and the formation of sulfuric acid in the atmosphere. The traditional view is that sulfur trioxide is removed by water vapor in the troposphere. However, the concentration of water vapor decreases significantly with increasing altitude, leading to longer atmospheric lifetimes of sulfur trioxide. Here, we utilize a dual-level strategy that combines transition state theory calculated at the W<sub>2</sub>X//DF-CCSD(T)-F12b/jun'-cc-pVDZ level, with variational transition state theory with small-curvature tunneling from direct dynamics calculations at the Mo8-HX/MG<sub>3</sub>S level. We also report the pressure-dependent rate constants calculated by using system-specific quantum Rice-Ramsperger-Kassel (SS-QRRK) theory. The present findings show that fall-off effects in the SO<sub>3</sub> + HONO<sub>2</sub> reaction are pronounced below 1 bar. The SO<sub>3</sub> + HONO<sub>2</sub> reaction can be a potential sink for SO<sub>3</sub> in the stratosphere and for HONO<sub>2</sub> in the troposphere, and the reaction can potentially compete well with the SO<sub>3</sub> + (H<sub>2</sub>O)<sub>2</sub> reaction between 25 and 35 km, as well as the OH + HONO<sub>2</sub> reaction. The present findings also suggest an unexpected new product from the SO<sub>3</sub> + HONO<sub>2</sub> reaction, which, although very short-lived, would have broad implications for understanding the partitioning of sulfur in the stratosphere, and the potential for the SO<sub>3</sub> reaction with organic acids to generate organosulfates without the need of heterogeneous chemistry.

Atmospheric SO<sub>3</sub> is an important intermediate in the formation of H<sub>2</sub>SO<sub>4</sub>, which is a critical component of acid rain, the stratospheric aerosol layer, new particle formation, and secondary aerosol.<sup>1-8</sup> The formation of gaseous H<sub>2</sub>SO<sub>4</sub> is initiated by the oxidation of SO<sub>2</sub> by the hydroxyl radical OH (R<sub>1</sub>), followed by the reaction of HOSO<sub>2</sub> with O<sub>2</sub> (R<sub>2</sub>).<sup>9,10</sup> The SO<sub>3</sub> produced by reactions (R<sub>1</sub>) and (R<sub>2</sub>) is expected to react with gaseous H<sub>2</sub>O, leading to gas phase H<sub>2</sub>SO<sub>4</sub>. The kinetics and mechanism of this reaction has been the subject of several laboratory studies.<sup>9-16</sup> The overall underlying chemistry is now referred to as the traditional acid rain scheme, shown below.<sup>17-</sup>



Results from a recent study<sup>21</sup> on the photochemistry of HOSO<sub>2</sub> suggest that the photochemical lifetime of the HOSO<sub>2</sub>

radical is around 70s, while the reactive lifetime of the HOSO<sub>2</sub> with O<sub>2</sub> is roughly 1 μs under Earth's stratospheric conditions.<sup>22</sup> Therefore, the photochemistry of the HOSO<sub>2</sub> radical will not compete with the O<sub>2</sub> reaction in the stratosphere. For SO<sub>3</sub>, the photochemistry has been addressed experimentally and theoretically. However, an examination of the lowest-lying singlet excited states of SO<sub>3</sub> indicates that the system is photostable under stratospheric conditions.<sup>21</sup> Once the photochemical stability of SO<sub>3</sub> is ensured, the efficiency of H<sub>2</sub>SO<sub>4</sub> generation from the association of SO<sub>3</sub> and H<sub>2</sub>O is only conditioned by largely unknown SO<sub>3</sub> removal processes. The findings from Carmona-García et al.<sup>21</sup> clearly point to a long photochemical lifetime of this molecule in the Earth's stratosphere, being roughly 579 days ( $J=2 \times 10^{-8} \text{ s}^{-1}$ ) at 16 km. Therefore, the only known reactive SO<sub>3</sub> sink is R<sub>3</sub>, which proceeds to form H<sub>2</sub>SO<sub>4</sub> at a rate of  $8.5 \times 10^{-4} \exp(+6540/T) [\text{H}_2\text{O}]^2 \text{ s}^{-1}$ ,<sup>23,24</sup> where there are two entrance channels SO<sub>3</sub> + H<sub>2</sub>O → H<sub>2</sub>O · H<sub>2</sub>O and SO<sub>3</sub> · H<sub>2</sub>O + H<sub>2</sub>O. Additional removal mechanisms of SO<sub>3</sub> are largely unknown and are the motivation of this work.

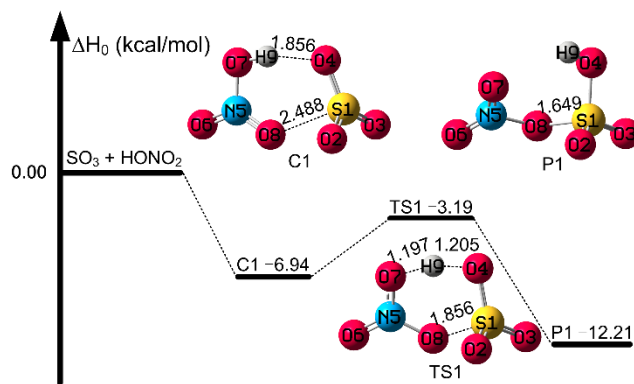


Figure 1. The calculated enthalpy profile at 0 K for the SO<sub>3</sub> + HONO<sub>2</sub> Reaction and the values at the W<sub>2</sub>X//DF-CCSD(T)-F12b/ jun'-cc-pVDZ level.

Here, we report theoretical work on a new reaction between SO<sub>3</sub> and nitric acid, which is potentially important because nitric acid has a relatively high concentration (in the range 10<sup>8</sup>-10<sup>9</sup> molecules cm<sup>-3</sup>), in the stratosphere:<sup>25</sup>



We have investigated R4 using the dual-level rate strategy developed by our group<sup>26</sup> that combines transition state theory at the W2X//DF-CCSD(T)-F12b<sup>28,29</sup>/jun'-cc-pVDZ level, with variational transition state theory including small-curvature tunneling<sup>30,31</sup> at the Mo8-HX/MG3S<sup>32,33</sup> level. The pressure-dependent rate constants are calculated using system-specific quantum Rice-Ramsperger-Kassel (SS-QRRK) theory;<sup>34</sup> the validity of this method was further shown by Master Equation<sup>35</sup> calculations in the SI (Supporting information). We have also computed the ultraviolet and visible (UV-Vis) absorption spectrum and cross sections of the final product of R4 by means of a well-established nuclear ensemble approach<sup>36-37</sup>, in conjunction with multi-state complete-active-space second-order perturbation theory (MS-CASPT2) method<sup>38-40</sup>. The resulting cross sections are then used to calculate the photodissociation rate ( $J/s^{-1}$ ) and subsequent photolysis lifetime of this product under stratospheric conditions. Detailed information is provided in the SI.

We have found two different reaction pathways for reaction R4, as shown in Figure S1. We only consider the much lower reaction pathway due to the big difference (about 28 kcal/mol) in the enthalpies of activation at 0 K. The reaction in the SO<sub>3</sub> + HONO<sub>2</sub> potential energy surface for the lower reaction pathway begins with the formation the pre-reactive C1 complex and proceeds to the transition state TS1 prior to the formation of product P1 (see Figure 1). Transition state TS1 corresponds to the transfer of the hydrogen atom (H9) from nitric acid to the oxygen atom (O4) of the sulfur trioxide, and simultaneous addition of the oxygen atom (O8) from nitric acid to the central sulfur atom (S1) of the sulfur trioxide, as shown in Figure 1. The O8-S1 bond length decreases from 2.488 Å in the pre-reactive complex C1 to 1.856 Å in the transition state, and the H9-O4 bond also shortens from 1.856 Å in C1 to 1.205 Å in TS1.

To provide further insight into the reaction mechanism, we also analyzed the natural orbitals of the transition state TS1. The results are provided in Figure S2, revealing that TS1 involves a hydrogen shift because the lone pair orbital of O8 in nitric acid is approximately perpendicular to the HONO<sub>2</sub> plane and cannot interact with the sulfur atom in SO<sub>3</sub>.

The enthalpy of activation at 0 K of R4 is -3.19 kcal/mol, calculated at W2X//DF-CCSD(T)-F12b/jun'-cc-pVDZ level (see Table S1). There is only 0.71 kcal/mol difference between the W2X//DF-CCSD(T)-F12b/jun'-cc-pVDZ and Mo8-HX/MG3S methods for the enthalpies of activation at 0 K. Therefore, Mo8-HX/MG3S has been used to do direct dynamics calculations. The calculated high-pressure-limit (HPL) rate constants are listed in Table S2 and fitted as analytic expression in SI.

The calculated activation energies are provided in Table S3. They show a strong negative temperature dependence, increasing from -3.83 kcal/mol at 190 K to -2.97 kcal/mol at 350 K. This temperature dependence is also shown by the rate constant of R4, which decreases with increasing temperature from

$6.18 \times 10^{-12} \text{ cm}^3 \text{ molecule}^{-1} \text{ s}^{-1}$  at 190 K to  $9.09 \times 10^{-14} \text{ cm}^3 \text{ molecule}^{-1} \text{ s}^{-1}$  at 350 K, as listed in Tables S2 and S3.

The pressure-dependent rate constants  $k_4(T, p)$  of reaction R4 are given in Table S4. The details of the determination of these values and the equations used<sup>41</sup> are described in the SI. The low-pressure limit rate constant  $k_{04}(T)$  is defined as the limit of  $k_4(T, p)/[\text{N}_2]$  when the pressure goes to zero. The calculated  $k_0(T)$  of R4 is  $9.34 \times 10^{-32} \text{ cm}^6 \text{ molecule}^{-2} \text{ s}^{-1}$  at 298 K. The fall-off effect, defined as the ratio  $k_{\infty 4}(T)/k_4(T, p)$  significantly increases with temperature as shown in Table S4 and Figure 2. For example,  $k_{\infty 4}(T)/k_4(T, p)$  at 1 bar increases from 1.02 at 200 K to 1.73 at 350 K. Figure 2 shows that the rate constant of R4 increases with increasing pressure below 1 bar. Table S5 shows that the ratio  $k_{\infty 4}(T)/k_{04}(T)$  is  $4.2 \times 10^7$  at 200 K and this ratio increases to  $5.4 \times 10^8$  at 350 K. The temperature dependence is more pronounced in the low-pressure limit rate constants than in the high-pressure limit ones. For example, between 200 and 350 K the calculated  $k_{04}(T)$  decreases by a factor of 528, compared with a factor of only 40 for  $k_{\infty 4}(T)$ . Of particular note is that fall-off effects are very large under stratospheric conditions: the pressure-dependent rate constant is predicted to be 96-458 times lower than the high-pressure limit rate constant between 40-50 km altitude (Table S7).

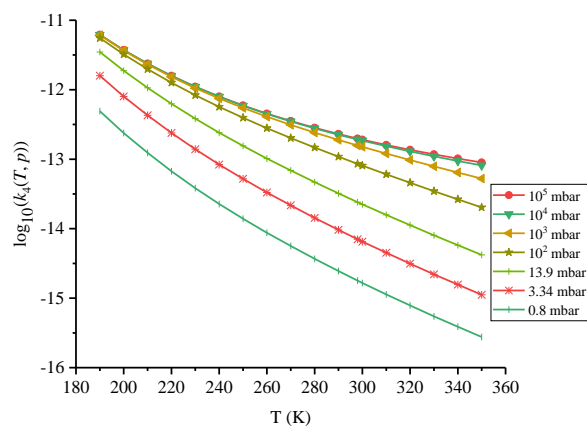


Figure 2. The rate constant of the SO<sub>3</sub> + HONO<sub>2</sub> reaction at different temperatures and pressures (bath gas: N<sub>2</sub>).

The transition pressure  $p_{1/2}$  is defined as the pressure where the pressure-dependent rate constant is half of the high-pressure limit rate constant. The transition pressure of reaction R4 as a function of temperature is plotted in Figure S3, showing positive correlation with temperature. In addition,  $p_{1/2}$  increases from 0.0136 bar at 200 K to 0.6596 bar at 350 K, which indicates that the pressure effect must be considered for reaction R4 (see Table S5).

Table 1. Atmosphere lifetimes (s) of the bimolecular reactions SO<sub>3</sub> + HONO<sub>2</sub> and SO<sub>3</sub> + (H<sub>2</sub>O)<sub>2</sub> and the concentration of HONO<sub>2</sub> and (H<sub>2</sub>O)<sub>2</sub> as functions of altitude.

| H <sup>a</sup><br>(km) | T <sup>a</sup><br>(K) | p <sup>a</sup><br>(mbar) | $k_4(T, p)^b$<br>(cm <sup>3</sup> molecule <sup>-1</sup> s <sup>-1</sup> ) | $k_3(T)^c$<br>(cm <sup>6</sup> molecule <sup>-2</sup> s <sup>-1</sup> ) | [HONO <sub>2</sub> ] <sup>a</sup><br>(molecules cm <sup>-3</sup> ) | [H <sub>2</sub> O] <sup>a</sup><br>(molecules cm <sup>-3</sup> ) | $\tau_{\text{HONO}_2}^d$<br>(s) | $\tau_{\text{H}_2\text{O}_2}^d$<br>(s) |
|------------------------|-----------------------|--------------------------|--|---|--|--|---------------------------------|--|
| 0                      | 290.2                 | 1013                     | $1.89 \times 10^{-13}$   | $4.69 \times 10^{-31}$  | $3.80 \times 10^8$   | $4.40 \times 10^{17}$  | $1.39 \times 10^4$              | $1.10 \times 10^{-5}$                  |
| 5                      | 250.5                 | 495.9                    | $5.05 \times 10^{-13}$   | $1.44 \times 10^{-29}$  | $1.50 \times 10^8$   | $1.70 \times 10^{16}$  | $1.32 \times 10^4$              | $2.40 \times 10^{-4}$                  |
| 10                     | 215.6                 | 242.8                    | $1.68 \times 10^{-12}$   | $8.52 \times 10^{-28}$  | $1.90 \times 10^9$   | $3.00 \times 10^{14}$  | $3.13 \times 10^2$              | $1.30 \times 10^{-2}$                  |

|    |       |       |                        |                        |                    |                       |                    |                       |
|----|-------|-------|------------------------|------------------------|--------------------|-----------------------|--------------------|-----------------------|
| 15 | 198   | 118.8 | $3.59 \times 10^{-12}$ | $1.16 \times 10^{-26}$ | $1.30 \times 10^9$ | $1.50 \times 10^{13}$ | $2.14 \times 10^2$ | $3.82 \times 10^{-1}$ |
| 20 | 208   | 58.18 | $1.92 \times 10^{-12}$ | $2.49 \times 10^{-27}$ | $5.50 \times 10^9$ | $4.20 \times 10^{12}$ | $9.48 \times 10^1$ | $2.27 \times 10^1$    |
| 25 | 216.1 | 28.48 | $1.05 \times 10^{-12}$ | $7.96 \times 10^{-28}$ | $4.60 \times 10^9$ | $2.50 \times 10^{12}$ | $2.08 \times 10^2$ | $2.01 \times 10^2$    |
| 30 | 221.5 | 13.94 | $5.82 \times 10^{-13}$ | $3.90 \times 10^{-28}$ | $2.30 \times 10^9$ | $1.50 \times 10^{12}$ | $7.47 \times 10^2$ | $1.14 \times 10^3$    |
| 35 | 228.1 | 6.826 | $2.65 \times 10^{-13}$ | $1.71 \times 10^{-28}$ | $5.80 \times 10^8$ | $8.90 \times 10^{11}$ | $6.50 \times 10^3$ | $7.39 \times 10^3$    |
| 40 | 240.5 | 3.341 | $8.17 \times 10^{-14}$ | $4.10 \times 10^{-29}$ | $5.70 \times 10^7$ | $4.80 \times 10^{11}$ | $2.15 \times 10^5$ | $1.06 \times 10^5$    |
| 45 | 251.9 | 1.636 | $2.50 \times 10^{-14}$ | $1.25 \times 10^{-29}$ | $2.50 \times 10^6$ | $2.50 \times 10^{11}$ | $1.60 \times 10^7$ | $1.28 \times 10^6$    |
| 50 | 253.7 | 0.801 | $1.17 \times 10^{-14}$ | $1.05 \times 10^{-29}$ | $1.60 \times 10^5$ | $1.20 \times 10^{11}$ | $5.34 \times 10^8$ | $6.61 \times 10^6$    |

<sup>a</sup>Data is from ref. 25.

<sup>b</sup>Rate constant of the  $\text{SO}_3 + \text{HONO}_2$  reaction ( $R_4$ ) at different temperature and pressure.

<sup>c</sup>Rate constant of the  $\text{SO}_3 + 2\text{H}_2\text{O}$  reaction ( $R_3$ ) from ref. 25.

<sup>d</sup> $\tau_{\text{HONO}_2}$  and  $\tau_{\text{H}_2\text{O}}$  are atmosphere lifetimes of  $\text{SO}_3$  for reaction with  $\text{HONO}_2$  and  $\text{H}_2\text{O}$ , respectively.

Our estimated atmospheric lifetimes for  $\text{SO}_3$  with respect to  $R_4$  from 0 km to 50 km are listed in Table 1. While the lifetime of  $\text{SO}_3$  with respect to  $R_4$  increases from 208 s at 25 km to 6500 s at 35 km ( $\text{SO}_3$  peaks in the atmosphere in this altitude range<sup>42</sup>), the lifetime with respect to  $R_3$  increases from 201 s at 25 km to 73900 s at 35 km. Hence, our calculations indicate that the  $\text{SO}_3 + \text{HONO}_2$  reaction should compete with the  $\text{SO}_3 + 2\text{H}_2\text{O}$  reaction over the altitude range between 25 km and 35 km. Outside this range, however, the atmospheric lifetime of  $\text{SO}_3$  with respect to  $R_4$  becomes significantly longer than that with respect to  $R_3$ , because of the large fall-off effects mentioned above. It should be noted that the atmospheric lifetime of  $\text{SO}_3$  in the troposphere is only  $10^{-5}$  s; nevertheless, field measurements still observe detectable  $\text{SO}_3$  concentrations.<sup>43</sup> In addition, we note that the rate constant for the  $\text{SO}_3 + \text{HONO}_2$  reaction is about 2 times faster than that of the  $\text{OH} + \text{HONO}_2$  reaction in Table S8. Typically, the concentration of  $\text{OH}$  is  $10^4$  to  $10^6$  molecule  $\text{cm}^{-3}$  and the concentration of  $\text{SO}_3$  can also reach  $10^6$  molecule  $\text{cm}^{-3}$  in the troposphere.<sup>43-48</sup> Therefore, the  $\text{SO}_3 + \text{HONO}_2$  reaction should be competitive with  $\text{OH} + \text{HONO}_2$ .

The product of reaction  $R_4$ ,  $\text{HOSO}_2\text{-NO}_3$ , is shown in Figure 1 as P1. Based on its computed UV-Vis absorption spectrum, displayed in Figure 3, the system only exhibits significant absorption at wavelengths shorter than 260 nm. Thus, the photolysis lifetime of P1 ranges from ~30 hours at 20 km to 12 minutes at 40 km, indicating that it should be relatively photostable under the stratospheric conditions considered. However, the thermal dissociation lifetime with respect to the reactants is around  $10^{-3}$ - $10^{-4}$  s in the stratosphere as shown in Table S9. By contrast, the lifetime of any reaction of P1 with  $\text{OH}$  in the stratosphere at the collision number ( $[\text{OH}] = 0.75$  pptv) would be on the order of 1500 s. These results suggest that the  $\text{SO}_3 + \text{HONO}_2$  reaction will introduce a new  $\text{HOSO}_2\text{-NO}_3$  product in the stratosphere that potentially partitions sulfur. The concentration of P1, from the  $\text{SO}_3 + \text{HONO}_2$  reaction, is distributed between 10-35 km as shown in Figure S4 (See SI). An increased  $\text{SO}_3$  represents a sensitivity exercise assuming the injection of large amounts of  $\text{SO}_3$ , e.g. 5 and 25 Tg(S)  $\text{yr}^{-1}$  to the stratosphere as proposed in some geoengineering<sup>49</sup> scenarios. Increasing  $\text{SO}_3$  in the stratosphere will increase the concentration of P1, suggesting that new partitioning of sulfur can occur because of the  $\text{SO}_3 + \text{HONO}_2$  reaction. This also raises new questions of what the chemical role and impact of P1 in stratospheric chemistry might be. Moreover, experimental observations have shown the existence of  $\text{NO}_3\text{SO}_3^-$  fragment in the stratosphere, which indirectly support the formation of the product P1 via  $\text{SO}_3$  reaction with  $\text{HONO}_2$ .<sup>49-50</sup> We also note that high levels of  $\text{SO}_3$  in Fig S4 has

relevance for Venus atmospheric sulfur chemistry and points to a new species of importance to this chemistry.

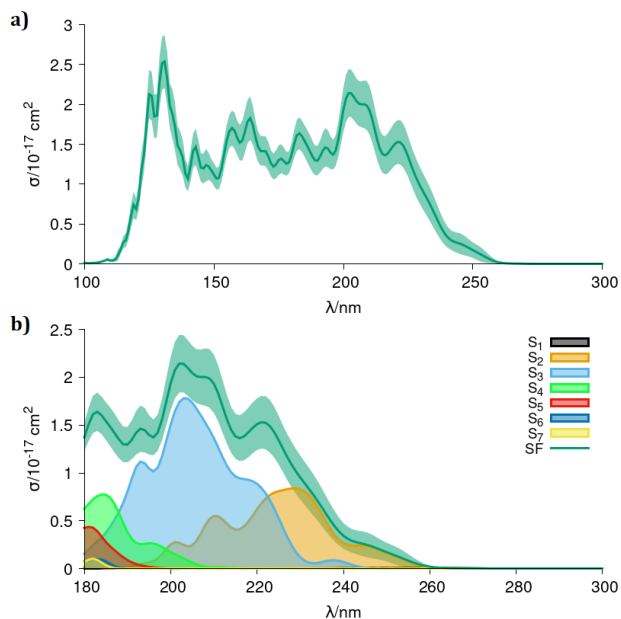


Figure 3. UV-Vis absorption spectrum and cross sections ( $\sigma/\text{cm}^2$ ) of the P1 product based on singlet spin-free (SF) electronic states (a and b), and contributions of the lowest-energy SF excited states S1-S7 (b). The light green areas correspond to the uncertainty of the cross section due to statistical sampling.

In summary, we find a new reaction route for sulfur trioxide in the stratosphere. This new reaction,  $\text{SO}_3 + \text{HONO}_2$ , brings new insights into our understanding of atmospheric sulfur chemistry. We also find that the falloff effect is an important parameter for controlling the atmospheric lifetimes of  $\text{SO}_3$  in the upper stratosphere by the  $\text{SO}_3 + \text{HONO}_2$  reaction. A final point is that this type of reaction may extend to other atmospheric acids such as carboxylic acids, potentially leading to the formation of organosulfates, previously considered to form via heterogeneous chemistry.<sup>51</sup>

## ASSOCIATED CONTENT

### Supporting Information

The Supporting Information is available free of charge on the ACS Publications website.

Computational methods, fitting of high-pressure-limit rate constant and calculated activation energies, fitting the pressure-dependent rate constant, the concentration of  $P_1$ , the calculated  $k(T, p)$  under different methods, the equilibrium constant, activation enthalpy and barrier height, tunneling transmission coefficients, high-pressure-limit rate constants ( $k_\infty(T)$  and activation energies ( $E_a$ ), Pressure-dependent  $k_4(T, p)$ , the fitted  $k_4(T, p)$  at different temperatures, the rate constant, atmospheric lifetimes, Cartesian coordinates, vibrational frequencies, the calculated enthalpy profile, the natural orbitals, and the transition pressure(PDF)

## AUTHOR INFORMATION

### Corresponding Author

Joseph S. Francisco – Department of Earth and Environmental Sciences and Department of Chemistry, University of Pennsylvania, Philadelphia, Pennsylvania 19104, United States; orcid.org/0000-0002-5461-1486; Email: frjoseph@sas.upenn.edu

### Authors

Bo Long – College of Materials Science and Engineering, Guizhou Minzu University, Guiyang 550025, China; orcid.org/0000-0002-9358-2585.

Yu Xia – College of Materials Science and Engineering, Guizhou Minzu University, Guiyang 550025, China

Junwei Lucas Bao – Department of Chemistry, Boston College, Chestnut Hill, Massachusetts 02467, United States; orcid.org/0000-0002-4967-663X

Javier Carmona-García – Institut de Ciència Molecular, Universitat de València, València 46071, Spain; Department of Atmospheric Chemistry and Climate, Institute of Physical Chemistry Rocasolano, CSIC, Madrid 28006, Spain; orcid.org/0000-0001-5359-7240

Juan Carlos Gómez Martín – Instituto de Astrofísica de Andalucía, CSIC, Granada 18008, Spain; orcid.org/0000-0001-7972-085X

John M. C. Plane – School of Chemistry, University of Leeds, LS2 9JT, Leeds, UK; orcid.org/0000-0003-3648-6893

Daniel Roca-Sanjuán – Institut de Ciència Molecular, Universitat de València, València 46071, Spain; orcid.org/0000-0001-6495-2770

Alfonso Saiz-Lopez – Department of Atmospheric Chemistry and Climate, Institute of Physical Chemistry Rocasolano, CSIC, Madrid 28006, Spain; orcid.org/0000-0002-0060-1581;

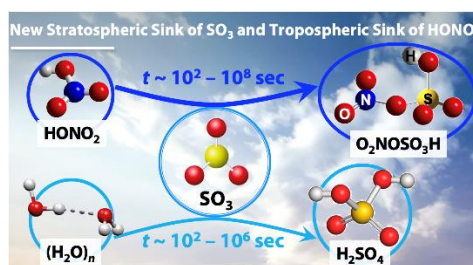
## Notes

The authors declare no competing financial interests.

## ACKNOWLEDGMENT

B.L. was supported in part by the National Natural Science Foundation of China (4210104007, 41775125, and 91961123), by the Science and Technology Foundation of Guizhou Province, China ([2019]5648), and by the Science and Technology Foundation of Guizhou Provincial Department of Education, China (KY[2021]014). The project that gave rise to these results received the support of a fellowship for J.C.-G. from “la Caixa” Foundation (ID 100010434); the fellowship code is LCF/BQ/DR20/11790027. D. R.-S. is thankful to the Spanish “Ministerio de Ciencia e Innovación (MICINN)” for funding (Project ref. CTQ2017-87054-C2-2-P, Unit of Excellence María de Maeztu CEX2019-000919-M and “Ramón y Cajal” grant RYC-2015-19234).

## TOC



## REFERENCES

- Larssen, T.; Lydersen, E.; Tang, D. G.; He, Y.; Gao, J. X.; Liu, H. Y.; Duan, L.; Seip, H. M.; Vogt, R. D.; Mulder, J.; Shao, M.; Wang, Y. H.; Shang, H.; Zhang, X. S.; Solberg, S.; Aas, W.; Okland, T.; Eilertsen, O.; Angell, V.; Li, Q. R.; Zhao, D. W.; Xiang, R. J.; Xiao, J. S.; Luo, J. H. Acid rain in China. *Environ. Sci. Technol.* **2006**, *40*, 418–425.
- Sipilä, M.; Berndt, T.; Petäjä, T.; Brus, D.; Vanhanen, J.; Stratmann, F.; Patokoski, J.; Mauldin, R. L.; Hyvärinen, A.-P.; Lihavainen, H.; Kulmala, M., The Role of Sulfuric Acid in Atmospheric Nucleation. *Science* **2010**, *327*, 1243–1246.
- Kulmala, M.; Kontkanen, J.; Junninen, H.; Lehtipalo, K.; Manninen, H. E.; Nieminen, T.; Petäjä, T.; Sipilä, M.; Schobesberger, S.; Rantala, P.; Franchin, A.; Jokinen, T.; Järvinen, E.; Äijälä, M.; Kangasluoma, J.; Hakala, J.; Aalto, P. P.; Paasonen, P.; Mikkilä, J.; Vanhanen, J.; Aalto, J.; Hakola, H.; Makkonen, U.; Ruuskanen, T.; Mauldin, R. L.; Duplissy, J.; Vehkamäki, H.; Bäck, J.; Kortelainen, A.; Riipinen, I.; Kurtén, T.; Johnston, M. V.; Smith, J. N.; Ehn, M.; Mentel, T. F.; Lehtinen, K. E. J.; Laaksonen, A.; Kerminen, V.-M.; Worsnop, D. R., Direct Observations of Atmospheric Aerosol Nucleation. *Science* **2013**, *339* (6122), 943–946.
- Bianchi, F.; Tröstl, J.; Junninen, H.; Frege, C.; Henne, S.; Hoyle, C. R.; Molteni, U.; Herrmann, E.; Adamov, A.; Bukowiecki, N.; Chen, X.; Duplissy, J.; Gysel, M.; Hutterli, M.; Kangasluoma, J.; Kontkanen, J.; Kürten, A.; Manninen, H. E.; Münch, S.; Peräkylä, O.; Petäjä, T.; Rondo, L.; Williamson, C.; Weingartner, E.; Curtius, J.; Worsnop, D. R.; Kulmala, M.; Dommen, J.; Baltensperger, U., New particle formation in the free troposphere: A question of chemistry and timing. *Science* **2016**, *352*, 1109–1112.
- Yao, L.; Garmash, O.; Bianchi, F.; Zheng, J.; Yan, C.; Kontkanen, J.; Junninen, H.; Mazon, S. B.; Ehn, M.; Paasonen, P.; Sipilä, M.; Wang, M.; Wang, X.; Xiao, S.; Chen, H.; Lu, Y.; Zhang, B.; Wang, D.; Fu, Q.; Geng, F.; Li, L.; Wang, H.; Qiao, L.; Yang, X.; Chen, J.; Kerminen, V.-M.; Petäjä, T.; Worsnop, D. R.; Kulmala, M.; Wang,

- L., Atmospheric new particle formation from sulfuric acid and amines in a Chinese megacity. *Science* **2018**, *361*, 278-281.
- 6 Chu, B.; Kerminen, V. M.; Bianchi, F.; Yan, C.; Petäjä, T.; Kulmala, M., Atmospheric new particle formation in China. *Atmos. Chem. Phys.* **2019**, *19*, 115-138.
  - 7 Chen, H.; Wang, M.; Yao, L.; Chen, J.; Wang, L., Uptake of Gaseous Alkylamides by Suspended Sulfuric Acid Particles: Formation of Ammonium/Aminium Salts. *Environ. Sci. Technol.* **2017**, *51*, 11710-11717.
  - 8 Kerminen, V.-M.; Chen, X.; Vakkari, V.; Petäjä, T.; Kulmala, M.; Bianchi, F., Atmospheric new particle formation and growth: review of field observations. *Environ. Res. Lett.* **2018**, *13*, 103003.
  - 9 Stockwell, W. R.; Calvert, J. G., The mechanism of the HO-SO<sub>2</sub> reaction. *Atmos. Environ.* **1983**, *17*, 2231-2235.
  - 10 Castleman, A. W., Jr., R. E. Davies, H. N. Munkelwitz, I. N. Tang, and P. Wood, Kinetics of association reactions pertaining to H<sub>2</sub>SO<sub>4</sub> aerosol formation, *Int. J. Chem. Kinet. Symp.* **1975**, *1*, 629-640.
  - 11 Wang, X.; Jin, Y. G.; Suto, M.; Lee, L. C.; O'Neal, H. E., Rate constant of the gas phase reaction of SO<sub>3</sub> with H<sub>2</sub>O. *J. Chem. Phys.* **1988**, *89*, 4853-4860.
  - 12 Reiner, T.; Arnold, F., Laboratory flow reactor measurements of the reaction SO<sub>3</sub> + H<sub>2</sub>O + M → H<sub>2</sub>SO<sub>4</sub> + M: Implications for gaseous H<sub>2</sub>SO<sub>4</sub> and aerosol formation in the plumes of jet aircraft. *Geophys. Res. Lett.* **1993**, *20*, 2659-2662.
  - 13 Reiner, T.; Arnold, F., Laboratory investigations of gaseous sulfuric acid formation via SO<sub>3</sub>+H<sub>2</sub>O+M→H<sub>2</sub>SO<sub>4</sub>+M: Measurement of the rate constant and product identification. *J. Chem. Phys.* **1994**, *101*, 7399-7407.
  - 14 Lovejoy, E. R.; Hanson, D. R.; Huey, L. G., Kinetics and Products of the Gas-Phase Reaction of SO<sub>3</sub> with Water. *J. Phys. Chem.* **1996**, *100*, 19911-19916.
  - 15 Kolb, C. E.; Jayne, J. T.; Worsnop, D. R.; Molina, M. J.; Meads, R. F.; Viggiano, A. A., Gas Phase Reaction of Sulfur Trioxide with Water Vapor. *J. Am. Chem. Soc.* **1994**, *116*, 10314-10315.
  - 16 Viggiano, A. A.; Arnold, F., Stratospheric sulfuric acid vapor: New and updated measurements. *Atmos. Environ.* **1983**, *88*, 1457-1462.
  - 17 Shepherd, J. G., Geoengineering the climate: an overview and update. *Phil. Trans. R. Soc. A* **2012**, *370*, 4166-4175.
  - 18 Pierce, J. R.; Weisenstein, D. K.; Heckendorn, P.; Peter, T.; Keith, D. W., Efficient formation of stratospheric aerosol for climate engineering by emission of condensable vapor from aircraft. *Geophys. Res. Lett.* **2010**, *37*, L18805.
  - 19 Crutzen, P. J., The possible importance of CSO for the sulfate layer of the stratosphere. *Geophys. Res. Lett.* **1976**, *3*, 73-76.
  - 20 Tuck, A. F.; Donaldson, D. J.; Hitchman, M. H.; Richard, E. C.; Tervahattu, H.; Vaida, V.; Wilson, J. C., On geoengineering with sulphate aerosols in the tropical upper troposphere and lower stratosphere. *Clim. Change* **2008**, *90*, 315-331.
  - 21 Carmona-García, J.; Trabelsi, T.; Francés-Monerris, A.; Cuevas, C. A.; Saiz-Lopez, A.; Roca-Sanjuán, D.; Francisco, J. S., Photochemistry of HOSO<sub>2</sub> and SO<sub>3</sub> and Implications for the Production of Sulfuric Acid. *J. Am. Chem. Soc.* **2021**, *143*, 18794-18802.
  - 22 Davis, D. D.; Ravishankara, A. R.; Fischer, S., SO<sub>2</sub> oxidation via the hydroxyl radical: Atmospheric fate of HSO<sub>x</sub> radicals. *Geophys. Res. Lett.* **1979**, *6*, 113-116.
  - 23 Jayne, J. T.; Pöschl, U.; Chen, Y.-m.; Dai, D.; Molina, L. T.; Worsnop, D. R.; Kolb, C. E.; Molina, M. J., Pressure and Temperature Dependence of the Gas-Phase Reaction of SO<sub>3</sub> with H<sub>2</sub>O and the Heterogeneous Reaction of SO<sub>3</sub> with H<sub>2</sub>O/H<sub>2</sub>SO<sub>4</sub> Surfaces. *J. Phys. Chem. A* **1997**, *101*, 10000-10011.
  - 24 Lovejoy, E. R.; Hanson, D. R.; Huey, L. G., Kinetics and Products of the Gas-Phase Reaction of SO<sub>3</sub> with Water. *J. Phys. Chem.* **1996**, *100*, 19911-19916.
  - 25 Basseur, G. P.; Solomon, S., *Aeronomy of the middle atmosphere: Chemistry and physics of the stratosphere and mesosphere*. Springer Science & Business Media: 2006; pp. 617-621
  - 26 Long, B.; Bao, J. L.; Truhlar, D. G., Atmospheric Chemistry of Criegee Intermediates: Unimolecular Reactions and Reactions with Water. *J. Am. Chem. Soc.* **2016**, *138*, 14409-14422.
  - 27 Chan, B.; Radom, L., W<sub>2</sub>X and W<sub>3</sub>X-L: Cost-Effective Approximations to W<sub>2</sub> and W<sub>4</sub> with kJ mol<sup>-1</sup> Accuracy. *J. Chem. Theory Comput.* **2015**, *11*, 2109-2119.
  - 28 Adler, T. B.; Knizia, G.; Werner, H.-J., A simple and efficient CCSD(T)-F12 approximation. *J. Chem. Phys.* **2007**, *127*, 221106.
  - 29 Knizia, G.; Adler, T. B.; Werner, H.-J., Simplified CCSD(T)-F12 methods: Theory and benchmarks. *J. Chem. Phys.* **2009**, *130*, 054104.
  - 30 Liu, Y. P.; Lynch, G. C.; Truong, T. N.; Lu, D. H.; Truhlar, D. G.; Garrett, B. C., Molecular Modeling of The Kinetic Isotope Effect for the [1,5]-Sigmatropic Rearrangement of cis-1,3-Pentadiene. *J. Am. Chem. Soc.* **1993**, *115*, 2408-2415.
  - 31 Bao, J. L.; Truhlar, D. G., Variational Transition State Theory: Theoretical Framework and Recent Developments. *Chem. Soc. Rev.* **2017**, *46*, 7548-7596.
  - 32 Zhao, Y.; Truhlar, D. G., Exploring the Limit of Accuracy of the Global Hybrid Meta Density Functional for Main-Group Thermochemistry, Kinetics, and Noncovalent Interactions. *J. Chem. Theory Comput.* **2008**, *4*, 1849-1868.
  - 33 Lynch, B. J.; Zhao, Y.; Truhlar, D. G., Effectiveness of Diffuse Basis Functions for Calculating Relative Energies by Density Functional Theory. *J. Phys. Chem. A* **2003**, *107*, 1384-1388.
  - 34 Bao, J. L.; Zheng, J.; Truhlar, D. G., Kinetics of Hydrogen Radical Reactions with Toluene Including Chemical Activation Theory Employing System-Specific Quantum RRK Theory Calibrated by Variational Transition State Theory. *J. Am. Chem. Soc.* **2016**, *138*, 2690-2704.
  - 35 Georgievskii, Y.; Miller, J. A.; Burke, M. P.; Klippenstein, S. J., Reformulation and Solution of the Master Equation for Multiple-Well Chemical Reactions. *J. Phys. Chem. A* **2013**, *117*, 12146-12154.
  - 36 Sitkiewicz, S. P.; Rivero, D.; Oliva-Enrich, J. M.; Saiz-Lopez, A.; Roca-Sanjuán, D., Ab initio quantum-chemical computations of the absorption cross sections of HgX<sub>2</sub> and HgXY (X, Y = Cl, Br, and I): molecules of interest in the Earth's atmosphere. *Phys. Chem. Chem. Phys.* **2019**, *21*, 455-467.
  - 37 Saiz-Lopez, A.; Sitkiewicz, S. P.; Roca-Sanjuán, D.; Oliva-Enrich, J. M.; Dávalos, J. Z.; Notario, R.; Jiskra, M.; Xu, Y.; Wang, F.; Thackray, C. P.; Sunderland, E. M.; Jacob, D. J.; Travníková, O.; Cuevas, C. A.; Acuña, A. U.; Rivero, D.; Plane, J. M. C.; Kinnison, D. E.; Sonke, J. E., Photoreduction of gaseous oxidized mercury changes global atmospheric mercury speciation, transport and deposition. *Nat. Commun.* **2018**, *9*, 4796.
  - 38 Roca-Sanjuán, D.; Aquilante, F.; Lindh, R., Multiconfiguration second-order perturbation theory approach to strong electron correlation in chemistry and photochemistry. *WIREs Comput. Mol. Sci.* **2012**, *2*, 585-603.
  - 39 Andersson, K.; Malmqvist, P. Å.; Roos, B. O., Second-order perturbation theory with a complete active space self-consistent field reference function. *J. Chem. Phys.* **1992**, *96*, 1218-1226.
  - 40 Finley, J.; Malmqvist, P.-Å.; Roos, B. O.; Serrano-Andrés, L., The multi-state CASPT<sub>2</sub> method. *Chem. Phys. Lett.* **1998**, *288*, 299-306.
  - 41 Long, B.; Bao, J. L.; Truhlar, D. G., Reaction of SO<sub>2</sub> with OH in the atmosphere. *Phys. Chem. Chem. Phys.* **2017**, *19*, 8091-8100.
  - 42 Gómez Martín, J. C.; Brooke, J. S. A.; Feng, W.; Höpfner, M.; Mills, M. J.; Plane, J. M. C., Impacts of meteoric sulfur in the Earth's atmosphere. *J. Geophys. Res.: Atmos.* **2017**, *122*, 7678-7701.
  - 43 Yao, L.; Fan, X.; Yan, C.; Kurtén, T.; Daellenbach, K. R.; Li, C.; Wang, Y.; Guo, Y.; Dada, L.; Rissanen, M. P.; Cai, J.; Tham, Y. J.; Zha, Q.; Zhang, S.; Du, W.; Yu, M.; Zheng, F.; Zhou, Y.; Kontkanen, J.; Chan, T.; Shen, J.; Kujansuu, J. T.; Kangasluoma, J.; Jiang, J.; Wang, L.; Worsnop, D. R.; Petäjä, T.; Kerminen, V.-M.; Liu, Y.; Chu, B.; He, H.; Kulmala, M.; Bianchi, F., Unprecedented Ambient Sulfur Trioxide (SO<sub>3</sub>) Detection: Possible Formation Mechanism and Atmospheric Implications. *Environ. Sci. Technol. Lett.* **2020**, *7*, 809-818.
  - 44 Seinfeld, J. H.; Pandis, S. N. *Atmospheric Chemistry and Physics*:

*From Air Pollution to Climate Change*, 2nd ed; Wiley-Interscience: New York, 2006, 204-209.

- 45 Yao, L.; Fan, X.; Yan, C.; Kurtén, T.; Daellenbach, K. R.; Li, C.; Wang, Y.; Guo, Y.; Dada, L.; Rissanen, M. P.; Cai, J.; Tham, Y. J.; Zha, Q.; Zhang, S.; Du, W.; Yu, M.; Zheng, F.; Zhou, Y.; Kontkanen, J.; Chan, T.; Shen, J.; Kujansuu, J. T.; Kangasluoma, J.; Jiang, J.; Wang, L.; Worsnop, D. R.; Petäjä, T.; Kerminen, V.-M.; Ren, X.; Harder, H.; Martinez, M.; Leshner, R. L.; Olliger, A.; Shirley, T.; Adams, J.; Simpas, J. B.; Brune, W. H. HO<sub>x</sub> concentrations and OH reactivity observations in New York City during PMTACS-NY 2001. *Atmos. Environ.* **2003**, *37*, 3627-3637.
- 46 Geyer, A.; Bächmann, K.; Hofzumahaus, A.; Holland, F.; Konrad, S.; Klüpfel, T.; Pätz, H.-W.; Perner, D.; Mihelcic, D.; Schäfer, H.-J.; Volz-Thomas, A.; Platt, U., Nighttime formation of peroxy and hydroxyl radicals during the BERLIOZ campaign: Observations and modeling studies. *J. Geophys. Res.: Atmos.* **2003**, *108*, 8249.
- 47 Stone, D.; Whalley, L. K.; Heard, D. E. Tropospheric OH and HO<sub>2</sub> radicals: field measurements and model comparisons. *Chem. Soc. Rev.* **2012**, *41*, 6348-6404.
- 48 Lelieveld, J.; Gromov, S.; Pozzer, A.; Taraborrelli, D. Global tropospheric hydroxyl distribution, budget and reactivity. *Atmos. Chem. Phys.* **2016**, *16*, 12477-12493.
- 49 Weisenstein, D. K.; Visionsi, D.; Franke, H.; Niemeier, U.; Vattioni, S.; Chiodo, G.; Peter, T.; Keith, D. W., An interactive stratospheric aerosol model intercomparison of solar geoengineering by stratospheric injection of SO<sub>2</sub> or accumulation-mode sulfuric acid aerosols. *Atmos. Chem. Phys.* **2022**, *22*, 2955-2973.
- 50 Reiner, T.; Arnold, F., Stratospheric SO<sub>2</sub>: Upper limits inferred from ion composition measurements - Implications for H<sub>2</sub>SO<sub>4</sub> and aerosol formation. *Geophys. Res. Lett.* **1997**, *24*, 1751-1754.
- 51 Schlager, H.; Arnold, F., Balloon-borne composition measurements of stratospheric negative ions and inferred sulfuric acid vapor abundances during the MAP/GLOBUS 1983 campaign. *Planet. Space Sci.* **1987**, *35*, 693-701.
- 52 Brüggemann, M.; Xu, R.; Tilgner, A.; Kwong, K. C.; Mutzel, A.; Poon, H. Y.; Otto, T.; Schaefer, T.; Poulain, L.; Chan, M. N.; Herrmann, H., Organosulfates in Ambient Aerosol: State of Knowledge and Future Research Directions on Formation, Abundance, Fate, and Importance. *Environ. Sci. Technol.* **2020**, *54*, 3767-3782.